RADAR SIGNALS

NADAV LEVANON
ELI MOZESON

A JOHN WILEY & SONS, INC., PUBLICATION

RADAR SIGNALS

RADAR SIGNALS

NADAV LEVANON
ELI MOZESON

A JOHN WILEY & SONS, INC., PUBLICATION

Published by John Wiley & Sons, Inc., Hoboken, New Jersey.
Published simultaneously in Canada.

Library of Congress Cataloging-in-Publication Data:

Levanon, Nadav.
Radar signals / Nadav Levanon, Eli Mozeson.
p. cm.
Includes bibliographical references and index.
ISBN 0-471-47378-2 (cloth)
1. Radar. I. Mozeson, Eli II. Title.

TK6575.L478 2004
621.3848–dc22
2003056882

Printed in the United States of America.

10 9 8 7 6 5 4 3 2 1

To the memory of my father Chaim Levanon,
who gave me two homes: our family and Tel Aviv University,
which he founded in 1953.

N.L.

To Dganit, Noam, and Nadav.

E.M.

CONTENTS

PREFACE

This book is devoted to the design and analysis of radar signals. The last comprehensive book dedicated to this subject was written in 1967 (Cook and Bernfeld; see Chapter 1 references). Since then, many journal and conference papers on radar signals have been published, as well as some good book chapters. Furthermore, the incredible progress in digital signal processing removed many of the constraints that squelched new signal ideas. Thus a new book on radar signals seems long overdue, and we believe that this book will fill the void.

Classical, enduring concepts such as the matched filter (Chapter 2) and the ambiguity function (Chapter 3) are discussed in detail, and useful related software is provided. Basic and advanced radar signals are described and analyzed. Many, if not most of the radar signals described in the open literature are presented and their performance analyzed. The knowledge gathered from these signals is used to suggest several new or modified signals that provide improved performance in resolution, ambiguity, spectral efficiency, and diversity.

The book contains tables of preferred signals and MATLAB codes for generating coded signals and for calculating and plotting ambiguity functions and other signal features. Each chapter is followed by a set of problems. Thus, the book can serve as a general reference as well as a textbook in an advanced radar course or a supplemental text in a basic radar course. In style and methodology it follows the approach used by Levanon in his 1988 text *Radar Principles* (see Chapter 1 references).

Following the chapters on matched filters and the ambiguity function, basic radar signals are discussed in Chapter 4 in terms of both analytical and numerical analysis. These include a constant-frequency pulse, a linear-FM pulse (with a weight window), and a coherent pulse train. Use of the MATLAB software provided is demonstrated using these simple signals.

In Chapter 5 we expand on other frequency-modulated schemes with detailed analysis of Costas coding and various nonlinear-FM signals. Chapter 6 provides a very comprehensive presentation of phase-coded signals, starting from Barker codes (binary and polyphase), minimum peak sidelobe codes, noiselike codes (PRNs), chirplike codes (Frank, Zadoff–Chu, P-codes), and codes suggested by Golomb, Ipatov, Huffman, and others. The chapter contains an important section on bandlimiting schemes in which the rectangular code element is replaced by a Gaussian windowed sinc or by a quadriphase waveform.

In Chapter 7 we expand on the most popular radar signal: a coherent train of linear-FM pulses. We offer a detailed analysis of its delay–Doppler performance, including intra- and interpulse weighting (matched or on-receive) for range and Doppler sidelobe reduction.

Diversity is widely used in radar signals, beginning with diversity of the pulse repetition interval (Chapter 8), which mitigates blind speeds. More elaborate diversity schemes are presented in Chapter 9, with emphasis on stepped-frequency pulses (both unmodulated and linear FM). The stepped-frequency signal is also used to demonstrate the important stretch-processing concept. The chapter ends with sections on complementary and orthogonal pulses.

Continuous-wave radar signals have experienced a revival in both military and civilian applications and are the subject of Chapter 10. Their analysis tool is the periodic ambiguity function, revisited in this chapter. Both analog and digital coded continuous-wave signals are presented and analyzed. Both matched-filter and simple mixer processing are studied.

Chapter 11 is devoted to multicarrier radar signals. Multicarrier is well known in communications but is a relatively new signal concept in radar. It offers the designer more degrees of freedom and more dimensions through which to introduce diversity. However, it entails variable amplitudes. Presently, this is a major hindrance in high-power amplifiers. But the aim of this book is to cover all worthy signals, including those that presently suffer from implementation difficulties.

In addition to the MATLAB programs embedded throughout the book, more elaborate MATLAB programs are provided in an appendix at the end of the book. Some of these programs include graphic user interfaces, which simplifies their use and allows quick change of parameters. Mastering the use of these programs is well worth the effort.

NADAV LEVANON
ELI MOZESON

1

INTRODUCTION

This book is devoted to the design and analysis of radar signals. Basic concepts such as the matched filter and the ambiguity function are discussed in detail, and useful related software is provided. Basic and advanced radar signals are presented and analyzed. The various chapters include many, if not most, of the radar signals described in the open literature. The knowledge obtained is utilized to suggest several new or modified signals with improved performance.

In the history of radar, signal ideas usually preceded implementation by many years, because of processing complexity and hardware limitations. In the introduction to their classical book *Radar Signals*, Cook and Bernfeld (1967) describe how the concept of pulse compression, developed and patented during World War II, was buried as a curiosity in the patent files. Only when the necessary transmitter components (e.g., high-power klystrons) became available did pulse compression win renewed interest.

In the first chapter of *Radar Design Principles*, Nathanson (1991) presents a checklist of possible constraints that can limit radar design. Among them are such questions as:

1. Can the transmitter support complex waveforms?
2. Is the transmitter suitable for pulsed- or continuous-wave transmission?
3. Are there unavoidable bandwidth limitations in the transmitter, receiver, or antenna?
4. Is frequency shifting from pulse to pulse practical?

Radar Signals, By Nadav Levanon and Eli Mozeson
ISBN 0-471-47378-2

Lack of coherent signal generation and amplification, which hampered pulse compression during World War II, seems naive today. So does the first item in Nathanson's checklist, dealing with complex waveforms. Extrapolating to the future, present limitations, such as the linear power amplifiers required for variable-amplitude radar signals, may raise eyebrows several years from now. In an attempt to extend its relevance, in this book we allow considerable freedom in the various characteristics of waveforms.

The word *Radar* (derived from "radio detection and ranging") summarizes the two main tasks of radar: detecting a target and determining its range. Fairly early range has expanded to include direction to the target and radial velocity between the radar and the target. Presently, more information on the target can be sought, such as its shape, size, and trajectory.

In most cases the reliability of detection, including the statistics of hits, misses, and false alarms, depends mostly on the signal's energy compared to the receiver's thermal noise level, and much less on the waveform. Determining the spatial direction to the target depends (in a stationary radar) on the antenna and its tracking system. The signal's waveform is responsible for the accuracy, resolution, and ambiguity of determining the range and radial velocity (range rate) of the target. Range is associated with the *delay* of the signal received. Range rate is associated with the *Doppler* shift of the signal received. These relationships are discussed next.

1.1 BASIC RELATIONSHIPS: RANGE–DELAY AND VELOCITY–DOPPLER

When the target can be approximated by a small point and the environment is free space, the relationship between range R and delay τ is simply

$$R = \tfrac{1}{2} C_{\mathrm{p}} \tau \tag{1.1}$$

where C_{p} is the velocity of propagation. The factor $\frac{1}{2}$ is due to the fact that the radar signal traverses the distance R twice (round trip). Equation (1.1) is only an approximation. In the lower atmosphere, C_{p} is not a constant but changes with altitude; hence the radar signal propagates a slightly longer distance along a bent path. Since the effect is minor and not very related to radar signals, it will be ignored.

The Doppler shift is developed in Box 1A with the help of Fig. 1.1, in which the propagation of two peaks (A and B) of a sinusoidal signal are followed as they propagate toward a target moving at a constant radial velocity v. It is shown that when the signal bandwidth is narrow compared with the carrier frequency (as in the case of a pure sinusoidal) and where the target radial velocity v is much smaller than the propagation velocity C_{p}, the *Doppler shift*, defined as the difference between the frequency received, f_{R}, and the frequency transmitted,

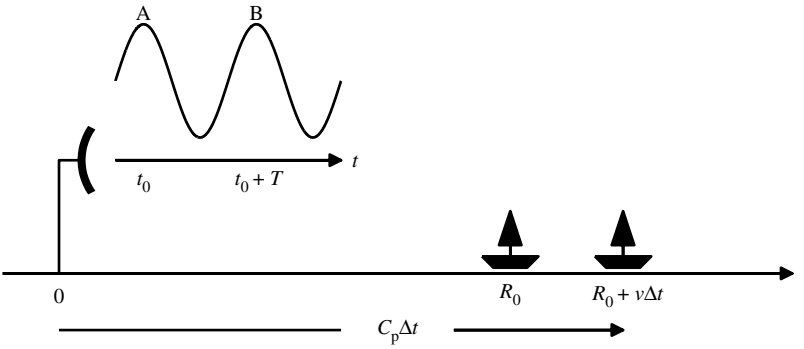

FIGURE 1.1 Timing in a Doppler scene.

BOX 1A: Doppler Effect

The Doppler shift is developed with the help of Fig. 1.1. Peak A departs at time $t = t_0$ when the target is at R_0 and reaches the target after travel time Δt, during which the target advanced an additional distance; hence,

$$C_p\ \Delta t = R_0 + v\ \Delta t \tag{1A.1}$$

where R_0 is the target location when peak A leaves the radar ($t = t_0$), Δt the travel time of peak A to reach the target, and $v\ \Delta t$ the distance advanced by target during Δt. Rewriting (1A.1), the signal's travel time is given by

$$\Delta t = \frac{R_0}{C_p - v} \tag{1A.2}$$

The moment t_1 in which peak A returns to the radar is given by

$$t_1 = t_0 + 2\ \Delta t = t_0 + \frac{2R_0}{C_p - v} \tag{1A.3}$$

Similar expressions can be worked out for the second peak B, which left the radar T seconds after peak A and returned at t_2:

$$t_2 = t_0 + T + \frac{2R_1}{C_p - v} \tag{1A.4}$$

where R_1 is the target location when peak B leaves the radar (at $t = t_0 + T$), t_2 the time of return of peak B to radar, and T the period of transmitted sinusoidal waveform. Note that R_1 in (1A.4) can be replaced by

$$R_1 = R_0 + vT \tag{1A.5}$$

The period of the received waveform T_R is equal to the difference between the arrival times of the two peaks:

$$T_R = t_2 - t_1 = t_0 + T + \frac{2(R_0 + vT)}{C_p - v} - \left(t_0 + \frac{2R_0}{C_p - v}\right) = T\frac{C_p + v}{C_p - v} \quad (1A.6)$$

The ratio between the received and transmitted periods is therefore

$$\frac{T_R}{T} = \frac{C_p + v}{C_p - v} \quad (1A.7)$$

and the ratio between the corresponding frequencies is

$$\frac{f_R}{f_0} = \frac{C_p - v}{C_p + v} = \frac{1 - v/C_p}{1 + v/C_p} \quad (1A.8)$$

yielding the received frequency,

$$f_R = f_0\frac{1 - v/C_p}{1 + v/C_p} \quad (1A.9)$$

In electromagnetic propagation (contrary to acoustic propagation) the expected target velocities are always much smaller than the velocity of propagation, $v \ll C_p$, yielding the approximation

$$\frac{1}{1 + v/C_p} = 1 - \frac{v}{C_p} + \frac{v^2}{C_p^2} - \cdots \quad (1A.10)$$

Using (1A.10) in (1A.9) yields

$$\begin{aligned} f_R &= f_0\left(1 - \frac{v}{C_p}\right)\left(1 - \frac{v}{C_p} + \frac{v^2}{C_p^2} - \cdots\right) \\ &= f_0\left(1 - \frac{2v}{C_p} + \cdots\right) \approx f_0\left(1 - \frac{2v}{C_p}\right) \end{aligned} \quad (1A.11)$$

Rewriting, we get

$$f_R \approx f_0 - \frac{2v}{C_p/f_0} = f_0 - \frac{2v}{\lambda} \quad (1A.12)$$

where λ is the wavelength transmitted. The Doppler shift is defined as

$$f_D = f_R - f_0 \approx -\frac{2v}{\lambda} \quad (1A.13)$$

f_0, is given by

$$f_D = f_R - f_0 \approx -\frac{2v}{\lambda} \tag{1.2}$$

where λ is the wavelength transmitted.

Figure 1.1 is a special case in which the velocity is exactly in the radial direction, hence equal to the range rate

$$v = \dot{R} \tag{1.3}$$

The more general approximation to the Doppler shift is therefore

$$f_D \approx -\frac{2\dot{R}}{\lambda} \tag{1.4}$$

The scenario depicted in Fig. 1.1 was also a special case from another point of view. The signal was a pure sinusoid at a frequency f_0. What happens when the signal contains modulation: that is, other frequencies? In other words, can we talk about a single Doppler shift when the signal has considerable bandwidth?

In wide (or ultrawide) bandwidth signals we have to go back to equation (1A.7) and note that the target's movement created a time scale between the signal transmitted and the signal received:

$$T = \frac{C_p - v}{C_p + v} T_R \underset{v \ll C_p}{\approx} \left(1 - \frac{2v}{C_p}\right) T_R \tag{1.5}$$

This time scale applies not only to the period of the signal but to the time axis in general. In other words, ignoring attenuation, the signal received, $s_R(t)$, can be written as a time-scaled and delayed version of the signal transmitted, $s(t)$:

$$s_R(t) = s\left[\left(1 - \frac{2v}{C_p}\right) t - \tau\right] \tag{1.6}$$

The delay τ is twice the one-way signal travel time Δt defined in (1A.2): namely,

$$\tau = 2\ \Delta t = \frac{2R_0}{C_p - v} = \frac{2R_0}{C_p(1 - v/C_p)} \approx \frac{2R_0}{C_p} \tag{1.7}$$

Errors resulting from the various approximations can be found in Appendix A of DiFranco and Rubin (1968). A popular rule of thumb says that if the signal bandwidth is less than one-tenth of the carrier frequency, the signal is considered a narrowband signal and it is reasonable to assume that the target motion causes only a Doppler shift of the carrier frequency according to (1.4). Otherwise, time scaling should be considered, which also affects the envelope of the signal. In the following chapters we use the narrowband assumption. Numerical simulations with rather complicated signals showed that the difference between the calculated

performances was very small, even when the narrowband assumption was used with a signal whose bandwidth reached 40% of the center frequency.

Another assumption made above and used henceforth is lack of radial acceleration: (i.e., $\ddot{R} \approx 0$). In most radar applications it is justified to assume that over the *coherently processed signal duration*, the radial velocity remains constant. In practice, the expected target acceleration is usually limited below some predetermined value characterizing the targets in question. The design of radar signals should take this value into consideration such that the target does not change its Doppler in an amount higher than Doppler resolution during the coherence processing period.

The phrases *coherently processed signal duration* and *Doppler resolution* need clarification. They can be explained with the example of a train of unmodulated pulses. As we will learn later in the book, Doppler resolution of a signal is a function of the total duration of the signal. A common approach to extending the signal is to repeat it periodically. A single pulse has poor Doppler resolution because the Doppler shift creates little change during the pulse duration. On the other hand, a train of pulses exhibits good Doppler resolution because of the changes (due to Doppler) between the pulses. This change is primarily in the Doppler-induced initial phase of each pulse. To extract this Doppler-induced phase change it is necessary for the receiver to know the original initial phase of each pulse. That is what we mean when we refer to the pulse train as a *coherent* pulse train. A simple example of a coherent pulse train is shown in Fig. 1.2.

The simple example in Fig. 1.2 is a special case in which the coherence was obtained by on–off switching of a continuous sinusoidal signal. However, any

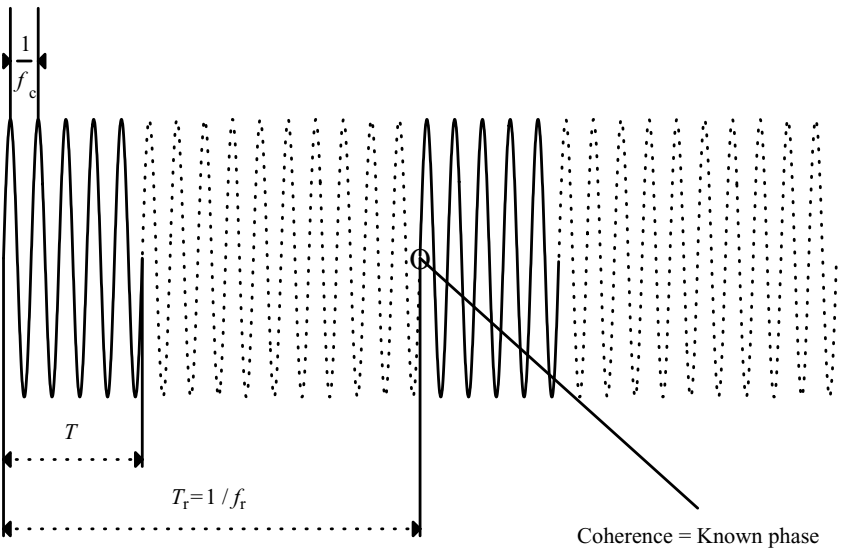

FIGURE 1.2 Coherent pulse train.

other initial phases (of the second and later pulses) are acceptable as long as the receiver knows what they were when transmitted. An example is radar utilizing a noncoherent transmitting device, where each transmitted pulse has a randomly generated initial phase. In such radar systems it is common to lock on the transmitted pulse phase using a dedicated circuit and to use this memorized phase as a reference for the pulse received. Implementations where the phase value is known only one pulse backward are usually referred to as *coherent on receive*.

Having associated range and velocity with two signal parameters, delay and Doppler, we can now discuss how well we can determine them and how the signal design can help.

1.2 ACCURACY, RESOLUTION, AND AMBIGUITY

Let us begin with a simple example. We need to measure the frequency of a sinusoidal signal. If the signal-to-noise-plus-interference ratio (SNIR) is very high (i.e., there are no other sinusoids and negligible random noise), we can measure the frequency with a counter. A counter counts the number of cycles within a given time span or measures the time interval between several zero crossings. A counter will produce an erroneous result when there is additive noise or when other sinusoidal signals are present: that is, when the signal-to-noise ratio (SNR) is low or when there are interferences from other signals. The lower the SNIR, the bigger the measurement error will be. Below a threshold SNIR, the counter will fail completely. What can be done in the low-SNIR scenario is to feed the received signal into many narrow bandpass filters, each centered at a different frequency. We can then find the filter that yields the highest output, or pick those filters whose outputs exceed a predetermined threshold. One way to implement such a bank of filters is to sample the input signal (plus noise) and perform fast Fourier transform (FFT).

The radar scenario is almost always a low-SNIR scenario. In some applications the radar performance is noise limited, while in other applications the performance is interference limited. The reflection from a target is almost always accompanied by reflections from the surrounding environment (ground, ocean), referred to as *clutter*, or by reflections from neighboring targets or targets farther away. For targets at a great distance or closer targets with a lower radar cross section (RCS), the thermal noise becomes a significant background. For this reason, measurements in radar are usually performed by a bank of filters, in delay and in Doppler.

Still, in many applications the target may stand alone and provide a high SNIR value (e.g., as in the case of ground-based antenna direction measurement of airborne targets). Indeed, in these cases it is practical to perform a measurement (e.g., angle measurement using the monopulse method) and not necessarily employ a multibeam array, which is equivalent to a bank of spatial filters. A more detailed discussion of measurement versus filtering in radar may be found in (Levanon, 1988).

The filter used in radar to measure the delay of a returned known signal is usually the matched filter. The matched filter is so important in radar that it is the subject of Chapter 2. The matched filter concentrates the entire energy of the signal into an output peak at a predetermined additional delay. It is therefore optimal for causing the output to cross the threshold and identify a detected reflection at the corresponding delay in the presence of the receiver thermal noise.

The peak of the output of a matched filter, when fed by the signal to which it was matched, is a function of the signal's energy and not of the signal's waveform. However, the output before and after the peak are strongly affected by the waveform. If the output level remains high over an extended delay, the threshold will be crossed in many delay cells, resulting in uncertainty as to which is the true delay. This implies that the measurement *accuracy* is proportional to the shape of the matched filter response close to the peak (actually, the second derivative of the response) and inversely proportional to the SNR.

Furthermore, if there are weaker neighboring targets that should be detected, their matched-filter output peak could be masked by a wide peak (mainlobe) or high sidelobes of a strong target. Thus the *resolution* or minimal separable distance (MSD) is proportional to the ambiguity function mainlobe width (usually measured at the -3 dB point) and inversely proportional to the SNIR. The interference level itself is a function of the nature of the interference. In a case where the interference is caused by a point target, the interference level is proportional to the interfering target RCS and the matched-filter sidelobe level expected at a given separation. The matched-filter peak sidelobe level ratio (PSLR) is often used to characterize the level of interference expected from point targets. For volume or surface clutter the interference level is characterized by the matched-filter integrated sidelobe level ratio (ISLR).

The science (or art) of designing radar signals is based on finding signals that yield a matched-filter response that matches a given application. For example, if closely separated targets are to be detected and distinguished in a low-SNR scenario, a radar signal having a matched-filter response that exhibits a narrow mainlobe (the peak) and low sidelobes is required. The mainlobe width and sidelobe level requirements are a function of the expected target separation and expected target RCS difference.

Two targets can be near each other in range (e.g., an aircraft flying over a patch of land) but way apart in radial velocity. For this reason radar receivers create filters matched not only to the signal transmitted but also to several different Doppler-shifted versions of it. Here again it is important to achieve a narrow response in Doppler, so that, for example, the moving target could be distinguished from the stationary background. Each one will cause a peak at a different Doppler-shifted matched filter. So the response of a matched filter needs to be studied in two dimensions: delay τ and Doppler ν. The tool for that is the ambiguity function (Woodward, 1953; Rihaczek, 1969), which describes that two-dimensional response. The ambiguity function $|\chi(\tau, \nu)|$ is the subject of Chapter 3. A basic question when designing a radar signal is: What is a good ambiguity function (AF), and can it be obtained? Intuitively, one could think

that the ideal AF should exhibit a single sharp peak at the origin (which is the nominal delay and Doppler for that matched filter), and near-zero level everywhere else (thumbtack shape). Even if it is the ideal AF, it cannot be produced completely. We learn in Chapter 3 that the AF peak at the origin cannot exceed a value of 1 and that the volume underneath the ambiguity function squared is a constant. If the AF is lowered in one area of the delay–Doppler plane, it must rise somewhere else.

Several AF shapes are presented in Figs. 1.3 to 1.6. Only two quadrants of the AF (positive Doppler) are plotted. Two adjacent quadrants contain all the information because the AF is symmetrical with respect to the origin. The four plots are presented in order to demonstrate different possible distributions of the AF volume over the delay–Doppler plane. The corresponding signals are discussed in more detail in later chapters of the book.

Figure 1.3 shows the AF of the most basic signal—an unmodulated pulse of width T (see Section 4.1). The delay axis is normalized with respect to T. The Doppler axis is normalized with respect to $1/T$. (The same type of normalization is used in Figs. 1.4 and 1.5.) The 0.5, 0.25, and 0.1 contour lines are also shown on top of the AF contour. The AF demonstrates the expected resolutions in delay and Doppler. The ambiguity function is zero for delays higher than the pulse width; thus no interference is expected with targets having range separation higher than the pulse duration. The ambiguity function shows relatively large sidelobes

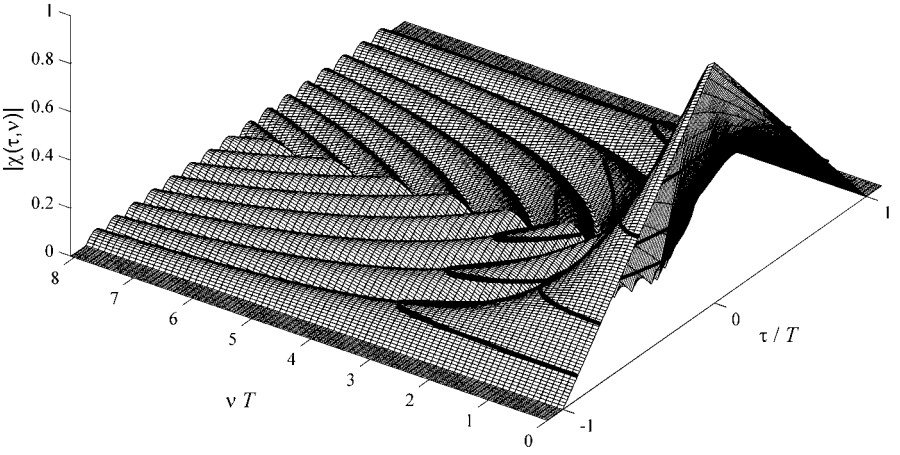

FIGURE 1.3 Ambiguity function of an unmodulated pulse.

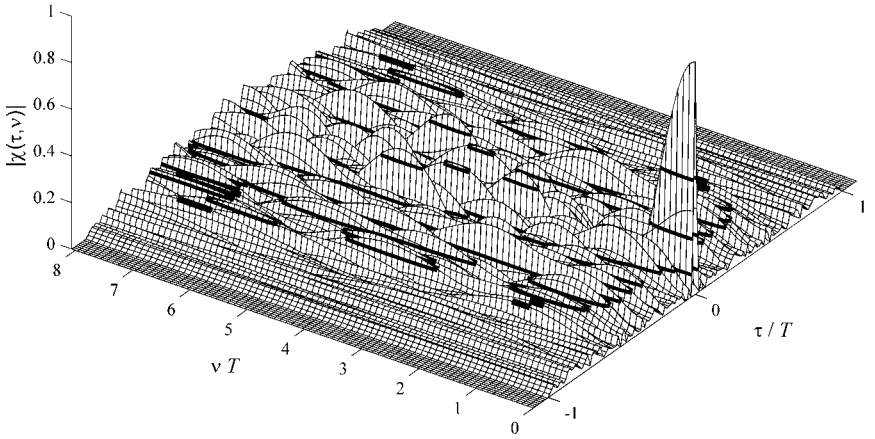

FIGURE 1.4 Ambiguity function of a minimum PSLR biphase pulse.

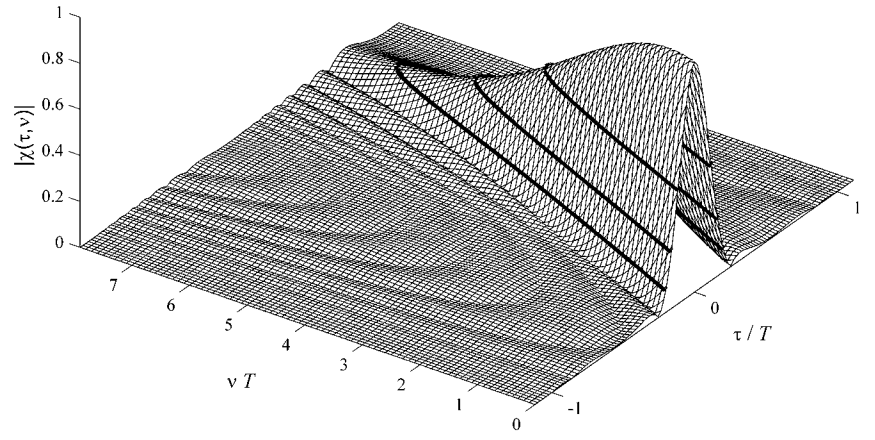

FIGURE 1.5 Ambiguity function of an amplitude-weighted linear-FM pulse.

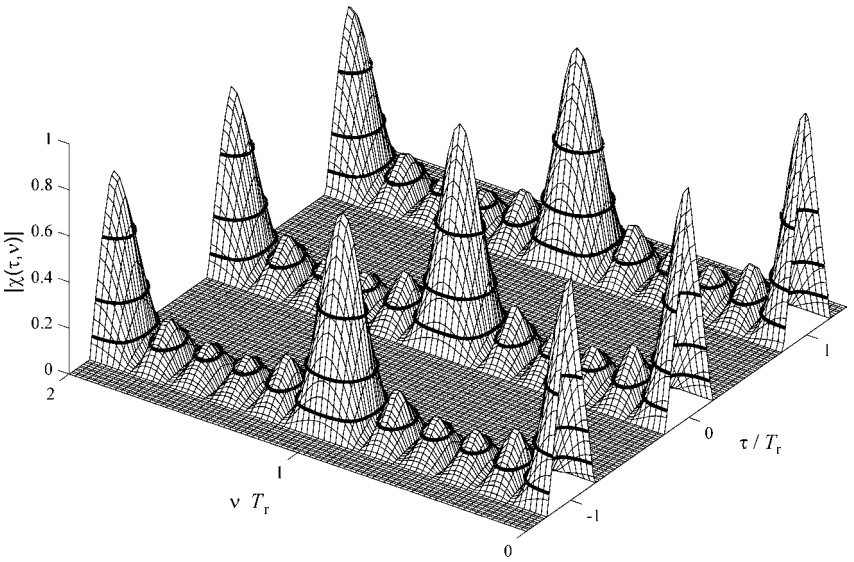

FIGURE 1.6 Ambiguity function of a train of six unmodulated pulses.

in Doppler (PSLR of -13 dB) and Doppler resolution of $1/T$ (both the -3 dB point separation and the first null are at $1/T$). Figure 1.3 is a poor approximation of a thumbtack shape using a signal with a time–bandwidth product of 1. (The time in the time–bandwidth product is the signal duration; the bandwidth is either the separation between the center frequency and the first spectral null or that between the two -3 dB frequencies.)

Figure 1.4 shows a better approximation of the thumbtack shape obtained with a very large time–bandwidth product by binary-phase modulating the pulse in a "random" way (a MPS 48-element biphase code was used; see Section 6.1.1). Similar ambiguity is also obtained by "randomly" frequency stepping the original pulse (using Costas codes; see Section 5.1). The time–bandwidth product used for the plot is 48 (the number of chips in the phase code). The normalized Doppler axis extends to only one-sixth of the time–bandwidth product, but a low sidelobe pedestal extends, in normalized Doppler, as far as the time–bandwidth product.

Signals with a large time–bandwidth product such as the one described here and the one used for Fig. 1.5 are also called *pulse compression waveforms*. The central spike of the AF (the waveform resolution cell size) has time duration $1/B$ and Doppler width $1/T$. The average height of the pedestal of the thumbtack function is $1/TB$, where TB is the time–bandwidth product (or *compression ratio*) of the signal. The AF is spread over a time interval T and a Doppler interval B. The total volume within the pedestal thus is 1, compared to a total volume of $1/TB$ in the central spike.

Figure 1.5 is the AF of a linear-FM pulse (see Section 4.2). The time–bandwidth product is 8. The normalized Doppler axis extends as far as that time–bandwidth product. The figure shows how increasing the bandwidth through modulation narrows (improves) the delay resolution, moving the AF volume from the vicinity of zero Doppler to higher Doppler shifts, yielding a ridge-shaped ambiguity function. Similar AF shapes are obtained by using ordered frequency or phase coding (e.g., P4 or Frank phase coding; see Section 6.2). The result of using "ordered" (in this case, linear) modulation is range–Doppler coupling, easily observed in the AF in the form of a diagonal ridge. Instead of a uniform sidelobe pedestal, the response energy is essentially concentrated at the area of the diagonal ridge, causing lower sidelobes outside the ridge.

Figure 1.6 is a periodic AF of a train of $N = 6$ unmodulated pulses with a duty cycle of $T/T_r = \frac{1}{5}$. (The *periodic* ambiguity function implies that the signal received is an infinitely long train of pulses, while the receiver coherently processes six pulses; see Section 4.3.) The plotted delay axis is normalized with respect to the pulse repetition interval T_r and extends over more than two periods. The Doppler axis plotted is normalized with respect to $1/T_r$ and extends as far as twice the repetition frequency. The figure shows a completely different AF shape in which the mainlobe at the origin is narrow along both the delay and the Doppler axis. The AF volume is now spread at many recurrent lobes, almost as high as the mainlobe at the origin. This shape is referred to as a *bed of nails*. This type of signal achieves good resolution in both delay and Doppler but creates both range and Doppler ambiguities. For example, a target at delay of $\tau + T_r$ will produce a response peak at exactly the same delay as a target at delay τ (usually referred to as *second-time-around echo* or *range folding*). Such an ambiguity is difficult to resolve.

Rihaczek (1971) identified and classified the four classes of ambiguity function described in Figs. 1.3 to 1.6. Table 1.1 summarizes the properties of the various classes, as can be observed from the corresponding AF plots. The constant volume under the ambiguity function squared puzzled many researchers and yielded several unfounded variations of the ambiguity function, which are no more than

TABLE 1.1 Waveform Classification and Ambiguity Functions

	Class			
	A	B1	B2	C
Figure	1.3	1.4	1.5	1.6
Time–bandwidth product	Unity	Large compared with unity		
Ambiguity function	Unsheared ridge	Thumbtack	Sheared ridge	Bed of nails
Resolution cell size	Unity	$1/TB$	Unity	$1/TB$
Ambiguities	No	No	Range–Doppler coupling	Spikes
Sidelobes	Low	High	Low	Low

mathematical fiction. Fourteen years after his book was published, Woodward attempted to dispose of some "grandiose clearance schemes." In a technical note of the Royal Radar Establishment (Woodward, 1967; Nathanson et al., 1991), Woodward wrote: "There is continued speculation on the subject of ambiguity clearance. Like slums, ambiguity has a way of appearing in one place as fast as it is made to disappear in another. That it must be conserved is completely accepted but the thought remains that ambiguity might be segregated in some unwanted part of the time–frequency plane where it will cease to be a practical embarrassment." Efficient (matched-filter) coherent processing of radar signals must obey the reality of the constant volume of AF squared. All the signal designer can do is to manipulate the AF volume so that it will best fit the expected radar target and its surrounding radar environment.

1.3 ENVIRONMENTAL DIAGRAM

The AF is an important tool in characterizing waveforms in terms of the resolution, sidelobe level, and ambiguity. The question of which ambiguity function should be preferred depends not only on the desired delay and Doppler resolution, or on the complexity of the required processor, but also on where the clutter or competing targets are located in the delay–Doppler plane (i.e., in the radar environment). Cook and Bernfeld (1967) stated that "in the extreme case, all signals (waveforms) are equally good (or bad) as long as they are not compared against a specific radar environment." In other words, when coming to the point of selecting a waveform (or waveform class) for a given radar application, the AF should be tested against the environmental parameters that characterize the application.

The environment that the radar encounters may consist of a variety of clutter conditions, countermeasure interference (such as chaff or deliberate electronic emissions), and interference from neighboring radars. The environmental diagram details spectral, spatial, and amplitude characteristics of the radar environment and is used as the basis against which the ambiguity diagram is played in selecting a waveform design. Nathanson et al. (1969) presented a basic model of a radar environmental diagram. An example of an environmental diagram of surveillance radar located at a coastal site is illustrated in Fig. 1.7. Radial velocity (Doppler) is given on the ordinate and the target extent (delay) is indicated along the abscissa. Diagrams such as Fig. 1.7 are sometimes referred to as *R–V diagrams* or *target space*. This environmental diagram shows only the regions in which land or sea clutter, rainstorm, and high-altitude chaff can be expected. The figure does not show their relative power level as seen by the radar. This additional information could be presented using a three-dimensional plot similar to an AF plot, taking into account the radar antenna pattern and direction of interest. For example, looking in the direction of the sea, the land clutter is received only through the antenna sidelobes (or even backlobes), whereas the sea clutter is in the mainlobe area.

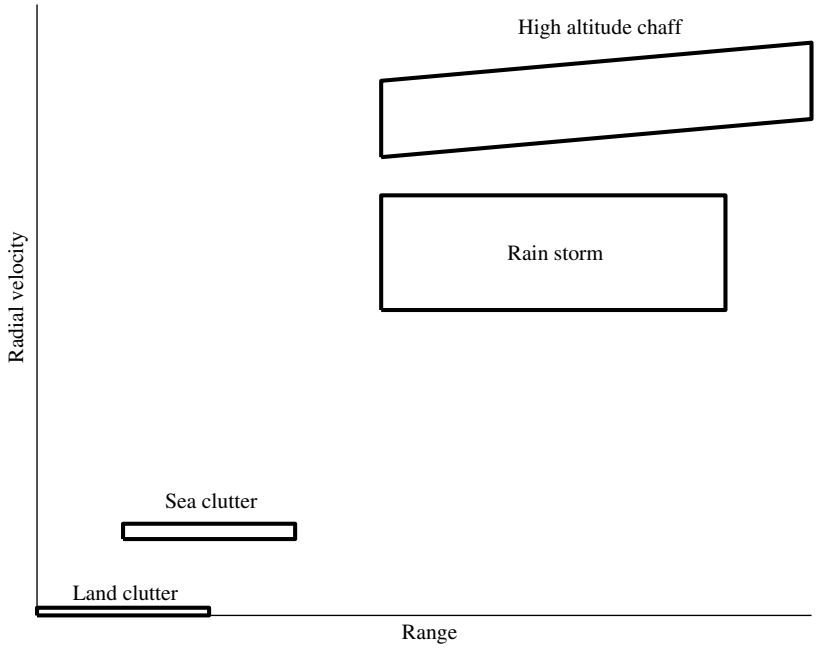

FIGURE 1.7 Basic environmental diagram of a coastal-based radar.

The basic environmental diagram gives a pictorial view of the clutter in range and velocity that the radar must contend with. By selecting the target trajectories expected within the R–V diagram and superimposing the ambiguity diagram of a particular waveform, it is possible to evaluate certain desirable characteristics inherent in the waveform. In Fig. 1.8 the AF contour of a pulse burst waveform is overlaid on the basic environmental diagram. As the target follows a particular trajectory, the ambiguity diagram will move accordingly, and AF ambiguous peaks will enter and exit the chaff and rainstorm space.

Aasen (1976) extended the concept of environmental diagrams to include other electromagnetic radiations from transmitters within the general locality of a radar site. Interference signals will appear to the radar receiver as signals with particular velocity and range characteristics. For example, a stable CW signal within the receiver bandwidth would appear as a horizontal straight line in an environmental diagram. If the CW signal were frequency modulated, the width of the line would increase according to the modulation bandwidth.

A different and far more complicated environmental diagram is of airborne radar. In this case the ground clutter is amplitude, range, and Doppler modulated due to the platform velocity, altitude, and antenna direction. The ground clutter appears in the environmental diagram in the form of a strong mainlobe clutter (MLC) caused by the antenna mainlobe illumination on a specific spot on the ground (limited in Doppler and delay) and a much weaker sidelobe clutter (SLC). The SLC extends in range from the minimal range determined by the platform